mathematics

MDPI

Article

Möbius-Coordinate Map Theorem for the Poincaré Disk

Watchareepan Atiponrat [1], Jaturon Wattanapan [2,3], Wanchalerm Sucpikarnon [1] and Teerapong Suksumran [1,*]

[1] Department of Mathematics, Faculty of Science, Chiang Mai University, Chiang Mai 50200, Thailand; watchareepan.a@cmu.ac.th (W.A.); wanchalerm.s@cmu.ac.th (W.S.)
[2] Office of Research Administration, Chiang Mai University, Chiang Mai 50200, Thailand; jaturon.w@cmu.ac.th
[3] Faculty of Science, Chiang Mai University, Chiang Mai 50200, Thailand
* Correspondence: teerapong.suksumran@cmu.ac.th

Abstract

We develop an explicit scalar coordinate treatment of the known orthogonal Möbius gyrodecomposition of the Poincaré disk. The Möbius real and imaginary parts express each point uniquely as an ordered Möbius sum of components on the Euclidean orthogonal real and imaginary diameters. The Möbius-Coordinate Map Theorem identifies the disk diffeomorphically with $(-1,1)^2$, and the coordinate parameters are bounded reparametrizations of Lobachevsky coordinates in a specified convention. We describe the associated equivalence classes: constant Möbius real part gives perpendicular hyperbolic lines, whereas nonzero constant Möbius imaginary part gives curves of constant signed distance from the real diameter. Rotational covariance supplies the formulas along arbitrary diameters. As a concrete application, the coordinates give the perpendicular foot and distance to a diameter directly from a disk point. The contribution is this explicit two-dimensional coordinate realization and its geometric interpretation, rather than a new general orthogonal decomposition theorem.

Keywords: hyperbolic geometry; Poincaré disk model; Möbius addition; hyperbolic line; gyrogroup

MSC: 51M09; 30F45; 20N05

1. Introduction

The Poincaré disk realizes the hyperbolic plane as the open unit disk of the complex plane [1,2]. Its hyperbolic lines are diameters or circular arcs orthogonal to the boundary circle, and its conformal metric preserves angles. Further accounts of this model and its relation to other models of hyperbolic geometry can be found in [3,4].

Gyrovector spaces provide an algebraic framework for hyperbolic geometry in which ordinary vector addition is replaced by operations such as Möbius addition and Einstein addition [5–7]. Although these operations are generally nonassociative, their algebraic identities allow geometric constructions to be expressed in terms of gyrogroup operations. The connection with relativistic velocity addition is developed in [8,9], while the relation between unit-ball geometry and Lorentz boosts is studied in [10]. Related hyperbolic structures also occur in the description of mixed-state qubit density matrices [11].

The gyrovector approach supports both geometric constructions and analysis. Hyperbolic barycentric calculus is treated in [12], with the triangle centroid providing a concrete example [13]. Möbius gyrovector methods also give a description of the hyperbolic square [14]. On the analytic side, a hyperbolic derivative in the Poincaré ball is introduced in

Check for updates

Academic Editor: Ruriko Yoshida

Received: 15 September 2026
Revised: 22 October 2026
Accepted: 27 October 2026
Published: 31 October 2026

Copyright: © 2026 by the authors. Licensee MDPI, Basel, Switzerland. This article is an open access article distributed under the terms and conditions of the Creative Commons Attribution (CC BY) license.

[15], and harmonic analysis on the Möbius gyrogroup is developed in [16]. A differential–geometric treatment of binary operations on the unit ball is given in [17]. These works provide broader context for expressing hyperbolic constructions algebraically; the present paper focuses on explicit orthogonal coordinates in the complex disk.

Ferreira and Suksumran [18] established orthogonal gyrodecompositions for real inner product gyrogroups, including the Möbius ball in arbitrary dimension, and developed the associated gyroprojections and partitions. Thus, the existence of a unique orthogonal Möbius representation and the general projection framework is already known. In the two-dimensional complex disk, these results can be expressed through two real scalar parameters. The question addressed here is how to write these parameters directly as functions of a disk point and use them to describe its coordinates, fibers, and elementary geometric calculations without first changing models.

Our contribution is an explicit coordinate treatment of this specialization. We derive scalar formulas for the Möbius real and imaginary parts, give a direct proof that they define a diffeomorphism from the disk to $(-1,1)^2$, identify the precise relation with Lobachevsky coordinates, and describe the two families of level sets. We also give formulas along rotated diameters and a worked calculation of perpendicular projection and distance to a diameter. The decomposition and the general-axis existence result are realizations of the known theory and rotational covariance, respectively; they are included to make the formulas and their use self-contained.

The coordinates are bounded reparametrizations of classical Lobachevsky coordinates, rather than a different hyperbolic geometry. Their useful feature here is their characterization by the ordered identity $z = r \oplus_M si$, with both r and s available explicitly in disk coordinates. This connects the algebraic representation to geometric projection and signed distance: one parameter determines the perpendicular foot, while the other determines distance from the chosen diameter. The resulting formulas also explain why the two coordinate families have different geometric behavior.

2. Preliminaries

The algebraic preliminaries follow the gyrogroup framework described in [5,19]. We specialize to the complex disk and collect basic definitions and notation below. Let $\mathbb{C}$ be the field of complex numbers. Let $\mathbb{D}$ be the open unit disk of $\mathbb{C}$; that is, $\mathbb{D} = \{z \in \mathbb{C} : |z| < 1\}$. Recall that *Möbius addition* is defined on the disk by

$$a \oplus_M b = \frac{a + b}{1 + \overline{a}b} \tag{1}$$

for all $a, b \in \mathbb{D}$. It turns out that the pair $(\mathbb{D}, \oplus_M)$ forms a nonassociative structure that shares several common properties with groups, known as the (complex) *Möbius gyrogroup*. In fact, the Möbius gyrogroup is a prominent example that motivates the theory of gyrogroups. Let $\mathbb{S}^1$ be the unit circle of the complex plane; that is, $\mathbb{S}^1 = \{\omega \in \mathbb{C} : |\omega| = 1\}$. Throughout the remainder of this article, $\mathbb{D}$ is referred to as the *Poincaré disk*. Möbius addition induces Möbius transformations on the Poincaré disk: for each $a \in \mathbb{D}$, define a function τ_a by $\tau_a(z) = a \oplus_M z$, called the *Möbius translation* induced by a. In fact, τ_a extends naturally to a Möbius transformation of the extended complex plane, given by the same formula.

We will use two identities that follow directly from Equation (1). First, Möbius addition is rotationally covariant:

$$\omega(a \oplus_M b) = (\omega a) \oplus_M (\omega b) \qquad \text{for all } \omega \in \mathbb{S}^1. \tag{2}$$

Indeed, $\overline{\omega a}\,\omega b = \overline{a}b$, and so both sides equal $\omega(a + b)/(1 + \overline{a}b)$. Second, left translation by $-a$ is the inverse of left translation by a:

$$(-a) \oplus_M (a \oplus_M b) = b \qquad \text{and} \qquad a \oplus_M ((-a) \oplus_M b) = b. \tag{3}$$

For the first identity, substituting $(a+b)/(1+\overline{a}b)$ gives numerator $(1-|a|^2)b/(1+\overline{a}b)$ and denominator $(1-|a|^2)/(1+\overline{a}b)$. The second identity follows by replacing a by $-a$. These identities keep the indicated parentheses and do not require associativity. Also,

$$1-|a\oplus_M b|^2=\frac{(1-|a|^2)(1-|b|^2)}{|1+\overline{a}b|^2}>0, \tag{4}$$

which proves closure in $\mathbb{D}$. On the real diameter, the operation is simply $u\oplus_M v=(u+v)/(1+uv)$ for all $u,v\in(-1,1)$.

Fix $a\in\mathbb{C}\setminus\{0\}$, and let $b\in\mathbb{C}$. Define the following transformations on the extended complex plane $\mathbb{C}\cup\{\infty\}$:

$$\rho_a(z)=\begin{cases} az & \text{if } z\in\mathbb{C};\\ \infty & \text{if } z=\infty;\end{cases}$$

$$T_b(z)=\begin{cases} z+b & \text{if } z\in\mathbb{C};\\ \infty & \text{if } z=\infty;\end{cases}$$

$$\kappa(z)=\begin{cases} \overline{z} & \text{if } z\in\mathbb{C};\\ \infty & \text{if } z=\infty;\end{cases}$$

$$\iota_{\mathbb{S}^1}(z)=\begin{cases} \dfrac{z}{|z|^2} & \text{if } z\in\mathbb{C}\setminus\{0\};\\ \infty & \text{if } z=0;\\ 0 & \text{if } z=\infty.\end{cases}$$

Let $a\in\mathbb{D}$ with $a\neq 0$. A direct computation shows that the Möbius translation τ_a can be factored as a composition:

$$\tau_a=T_{\frac{a}{|a|^2}}\circ\rho_{\frac{|a|^2-1}{|a|^2}a}\circ\kappa\circ\iota_{\mathbb{S}^1}\circ T_1\circ\rho_{\overline{a}}. \tag{5}$$

This factorization provides a visualization of a translated diameter in Section 4. In fact, applying the factors to z gives successively $\overline{a}z$, $1+\overline{a}z$, $1/(1+\overline{a}z)$ after inversion and conjugation, and finally

$$\frac{a}{|a|^2}+\frac{(|a|^2-1)a}{|a|^2(1+\overline{a}z)}=\frac{a+z}{1+\overline{a}z}.$$

The factorization is not needed for the Coordinate-Map Theorem in Section 3. Its role is to illustrate the standard geometric action of the left translations that describe the projection fibers in Section 4.

3. Orthogonal Decomposition in the Poincaré Disk

Factorizations of Möbius gyrogroups have been studied in [20,21], and orthogonal gyroexpansions are developed in [22]. The general orthogonal gyrodecomposition underlying our construction is established in [18]. In this section, we derive the scalar coordinate functions $M_{\mathfrak{R}}$ and $M_{\mathfrak{I}}$ and prove that their ordered reconstruction map gives global smooth coordinates on the Poincaré disk. The distinction between these coordinate functions and gyrogroup homomorphisms is clarified below using the classification in [23]. For each $\omega\in\mathbb{S}^1$, define

$$L_\omega=\{t\omega : t\in\mathbb{R}, -1<t<1\}. \tag{6}$$

For $u,v\in(-1,1)$, note that

$$(u\omega)\oplus_M(v\omega)=\frac{u+v}{1+uv}\omega,\qquad -(u\omega)=(-u)\omega.$$

Moreover, $1 - ((u+v)/(1+uv))^2 = (1-u^2)(1-v^2)/(1+uv)^2 > 0$. Thus, L_ω is closed under Möbius addition and negation and hence is a subgyrogroup of $(\mathbb{D}, \oplus_M)$. In the case when $\omega = 1$, we recover the diameter of the Poincaré disk lying on the real axis. In the case when ω is the imaginary unit i, we recover the diameter of the Poincaré disk lying on the imaginary axis. Indeed, L_ω represents a hyperbolic line in the Poincaré disk model for it is a diameter of the disk. The following theorem states that each complex number in the Poincaré disk can be decomposed uniquely as a Möbius sum of a real number in L_1 and a purely imaginary number in L_i. This resembles the fact that each complex number z can be decomposed uniquely as a sum of a real number and a purely imaginary number in the usual way, namely $z = \mathrm{Re}(z) + \mathrm{Im}(z)i$.

Theorem 1. *If z is a complex number in the Poincaré disk, then there is a unique pair (r, w) in $L_1 \times L_i$ such that $z = r \oplus_M w$.*

Proof. Write $z = x + yi$, set $q = x^2 + y^2$, and set $\Delta = \sqrt{(1+q)^2 - 4x^2}$. Then, $q < 1$ and $\Delta = \sqrt{(1-q)^2 + 4y^2}$. Since $\Delta \geq 1 - q > 0$, we can define

$$r = \frac{2x}{1+q+\Delta}, \qquad w = (-r) \oplus_M z.$$

Note that the denominator defining r is at least 2, and so $|r| \leq |x| < 1$. Hence, w is well-defined and lies in $\mathbb{D}$ by the closure property of Möbius addition noted after Equation (4). Hence, the identity $x(1+r^2) - r(1+q) = 0$ follows by considering the quadratic equation $xt^2 - (1+q)t + x = 0$ in the variable t and is immediate when $x = 0$. On multiplying numerator and denominator in $(-r+z)/(1-rz)$ by $1 - r\bar{z}$, we consequently obtain that

$$\mathrm{Re}(w) = \frac{x(1+r^2) - r(1+q)}{|1-rz|^2} = 0.$$

Since $w \in \mathbb{D}$, it follows that $w = si$ for some $s \in (-1, 1)$. Equation (3) now gives $z = r \oplus_M si$. Comparing imaginary parts of $z(1+rsi) = r + si$ gives $y = s(1-rx)$. Note that $1 - rx \neq 0$ since otherwise $|r||x| = 1$, a contradiction. Therefore, the second parameter is explicitly $s = \dfrac{2y}{1-q+\Delta}$. These expressions include the cases $x = 0$ or $y = 0$ without separate definitions.

For uniqueness, suppose that $z = u \oplus_M vi$ with $u, v \in (-1, 1)$. By left cancellation, $(-u) \oplus_M z = vi$, and so its real part vanishes and $xu^2 - (1+q)u + x = 0$. If $x = 0$, this forces $u = 0 = r$. If $x \neq 0$, the above value r is one root and the other root is $1/r$, which has absolute value greater than 1. Thus, $u = r$ is the only admissible root. Finally, cancellation gives $vi = (-r) \oplus_M z = si$, and so $v = s$. This proves existence and uniqueness. □

Indeed, Theorem 1 admits a broader scope, as its validity extends to more general axes, a result established in the following proposition.

Proposition 1. *Let $\omega \in \mathbb{S}^1$. If z is a complex number in the Poincaré disk, then there is a unique pair (u, v) in $L_\omega \times L_{\omega i}$ such that $z = u \oplus_M v$.*

Proof. Let $z \in \mathbb{D}$. Then, $z/\omega \in \mathbb{D}$. By Theorem 1, $z/\omega = r \oplus_M si$ for some $r, s \in (-1, 1)$. Hence, by Equation (2), $z = r\omega \oplus_M s\omega i$. This proves the existence part. Now, assume that $z = u \oplus_M v$ with $u \in L_\omega$ and $v \in L_{\omega i}$. Then, $u = t_1\omega$ and $v = t_2\omega i$ for some $t_1, t_2 \in (-1, 1)$. It follows that

$$\frac{z}{\omega} = \frac{u}{\omega} \oplus_M \frac{v}{\omega} = t_1 \oplus_M t_2 i,$$

and so $t_1 = r$ and $t_2 = s$ by the uniqueness part of Theorem 1. □

https://doi.org/10.3390/math14213971

Let $\omega \in \mathbb{S}^1$. If $t\omega = u\omega i$ with $t, u \in \mathbb{R}$, then $t = ui$, and so $t = u = 0$. This shows that $L_\omega \cap L_{\omega i} = \{0\}$. Furthermore,

$$\langle t\omega, u\omega i\rangle = \frac{1}{2}(-tui + tui) = 0,$$

where $\langle z, w\rangle = \frac{1}{2}(z\overline{w} + \overline{z}w)$ is the Euclidean inner product on $\mathbb{C} \cong \mathbb{R}^2$. Orthogonality of the factors always refers to this inner product. The notation $\mathbb{D} = L_\omega \oplus_M L_{\omega i}$ means that each point has a unique ordered representation with one factor in each diameter; it is not a vector-space direct sum.

This is precisely the two-dimensional specialization of the orthogonal gyrodecomposition in [18] (Section 4.2, Theorem 22). To identify the projection maps explicitly, take the Euclidean subspace $U = \mathbb{R} \subset \mathbb{C}$ and its orthogonal complement $U^\perp = i\mathbb{R}$. The corresponding ordered decomposition has factors in $U \cap \mathbb{D} = L_1$ and $U^\perp \cap \mathbb{D} = L_i$. Uniqueness identifies those factors with r and si in the preceding proof. Hence, the factor-selecting gyroprojectors are represented by $M_\mathfrak{R}(z)$ and $M_\mathfrak{I}(z)i$, respectively, once the scalar functions below are defined. More generally, $U = \omega\mathbb{R}$ gives the rotated projections in Section 4.

The comparison extends to the coefficients themselves. In the Möbius-ball specialization of [18] (Theorem 22, Equations (62) and (63)), the factors associated with the ordinary orthogonal components $u = x$ and $v = yi$ have the form $\lambda_1 u$ and $\lambda_2 v$. With $q = x^2 + y^2$ and $\Delta = \sqrt{(1-q)^2 + 4y^2}$, their nonzero-component formulas specialize to

$$\lambda_1 = \frac{2}{1+q+\Delta} \quad \text{and} \quad \lambda_2 = \frac{2}{1-q+\Delta}.$$

Thus, $r = \lambda_1 x$ and $si = \lambda_2 yi$, and the scalar formulas below agree with those general factors, including their continuous values on the axes. Their algebraic form is not claimed to be independent of the known decomposition formulas. Our treatment packages these factors as global scalar coordinates in the disk and develops their coordinate and geometric interpretation.

Using the identity

$$\sqrt{(1-|z|^2)^2 + 4\mathrm{Im}(z)^2} = \sqrt{(1+|z|^2)^2 - 4\mathrm{Re}(z)^2},$$

we express the parameters from Theorem 1 as scalar functions $M_\mathfrak{R}$ and $M_\mathfrak{I}$ on the Poincaré disk:

$$M_\mathfrak{R}(z) = \frac{2\mathrm{Re}(z)}{1+|z|^2+\sqrt{(1+|z|^2)^2 - 4\mathrm{Re}(z)^2}} \tag{7}$$

and

$$M_\mathfrak{I}(z) = \frac{2\mathrm{Im}(z)}{1-|z|^2+\sqrt{(1-|z|^2)^2 + 4\mathrm{Im}(z)^2}}. \tag{8}$$

The existence calculation in Theorem 1 identifies these values with r and s and gives

$$z = M_\mathfrak{R}(z) \oplus_M M_\mathfrak{I}(z)i \tag{9}$$

for all $z \in \mathbb{D}$. Therefore, $M_\mathfrak{R}(z)$ is referred to as the *Möbius real part* of z, and $M_\mathfrak{I}(z)$ is referred to as the *Möbius imaginary part* of z. Note that $M_\mathfrak{R}$ and $M_\mathfrak{I}$ are indeed functions from the Poincaré disk $\mathbb{D}$ to the open interval $(-1, 1)$. Moreover, according to Theorem 4 of [23], $M_\mathfrak{R}$ and $M_\mathfrak{I}$ are never gyrogroup homomorphisms. Figure 1 demonstrates a point z in the Poincaré disk described by the Cartesian coordinate system compared with the aforementioned Möbius coordinate system.

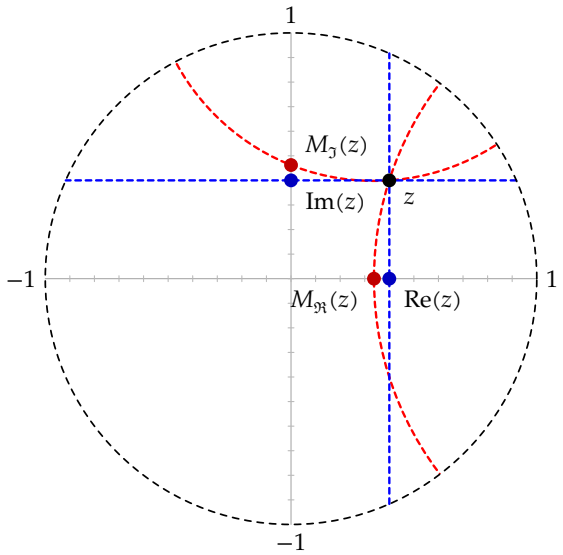

Figure 1. A point $z = \mathrm{Re}(z) + \mathrm{Im}(z)i$ in the Poincaré disk of the complex plane that can be expressed as a Möbius sum $z = M_{\Re}(z) \oplus_M M_{\mathfrak{I}}(z)i$. The blue dashed lines represent Euclidean lines in the complex plane, whereas the red dashed lines represent hyperbolic lines in the Poincaré disk.

The functions $M_{\Re}$ and $M_{\mathfrak{I}}$ can be interpreted as projection functions in the sense of the following proposition.

Proposition 2. *Let $z \in \mathbb{D}$, and let $s, t \in (-1, 1)$. Then, $M_{\Re}(M_{\Re}(z) \oplus_M si) = M_{\Re}(z)$ and $M_{\mathfrak{I}}(t \oplus_M M_{\mathfrak{I}}(z)i) = M_{\mathfrak{I}}(z)$.*

Proof. Set $w = M_{\Re}(z) \oplus_M si$. By construction, $w = M_{\Re}(w) \oplus_M M_{\mathfrak{I}}(w)i$. By the uniqueness part of Theorem 1, $M_{\Re}(w) = M_{\Re}(z)$, and so $M_{\Re}(M_{\Re}(z) \oplus_M si) = M_{\Re}(z)$. For the second identity, let $w = t \oplus_M M_{\mathfrak{I}}(z)i$. Both $(t, M_{\mathfrak{I}}(z)i)$ and $(M_{\Re}(w), M_{\mathfrak{I}}(w)i)$ are pairs in $L_1 \times L_i$ representing w. Uniqueness therefore gives $M_{\mathfrak{I}}(z) = M_{\mathfrak{I}}(w) = M_{\mathfrak{I}}(t \oplus_M M_{\mathfrak{I}}(z)i)$, as required. □

In view of Equations (7) and (8), note that $M_{\Re}(\bar{z}) = M_{\Re}(z)$ and $M_{\mathfrak{I}}(\bar{z}) = -M_{\mathfrak{I}}(z)$ for all $z \in \mathbb{D}$. The following theorem shows that there is a one-to-one correspondence between the points in the Poincaré disk and the set of all pairs (r, s) in $(-1, 1)^2$.

Theorem 2 (Möbius-Coordinate Map Theorem)**.** *Equip the open sets $\mathbb{D} \subset \mathbb{C} \cong \mathbb{R}^2$ and $(-1, 1)^2 \subset \mathbb{R}^2$ with their usual smooth structures. The map*

$$\Phi : \mathbb{D} \longrightarrow (-1, 1)^2, \qquad \Phi(z) = (M_{\Re}(z), M_{\mathfrak{I}}(z)),$$

is a diffeomorphism with inverse

$$\Psi : (-1, 1)^2 \longrightarrow \mathbb{D}, \qquad \Psi(r, s) = r \oplus_M si.$$

Proof. Theorem 1 shows that Φ takes values in $(-1, 1)^2$, and Equation (4) shows that Ψ takes values in $\mathbb{D}$. Reconstruction gives $\Psi(\Phi(z)) = z$ for all $z \in \mathbb{D}$. Conversely, uniqueness of the representation of $r \oplus_M si$ with $r, s \in (-1, 1)$ gives $\Phi(\Psi(r, s)) = (r, s)$. Therefore, $\Psi \circ \Phi = I_{\mathbb{D}}$ and $\Phi \circ \Psi = I_{(-1,1)^2}$, where $I_X : X \to X$ denotes the identity map on X.

For smoothness, write $z = x + yi$, and assume that $q = x^2 + y^2 < 1$. The two radicands in Equations (7) and (8) are equal:

$$(1 + q)^2 - 4x^2 = (1 - q)^2 + 4y^2 > 0.$$

Their positive square root is a smooth function of (x, y) on $\mathbb{D}$. Moreover, the denominators $1 + q + \sqrt{(1-q)^2 + 4y^2}$ and $1 - q + \sqrt{(1-q)^2 + 4y^2}$ are strictly positive. Hence, Φ is smooth. Finally, using Formula (1), one obtains that

$$\Psi(r, s) = \frac{r(1+s^2)}{1+r^2s^2} + \frac{s(1-r^2)}{1+r^2s^2}i,$$

and so Ψ is smooth on $(-1, 1)^2$ because $1 + r^2s^2 > 0$. Therefore, the mutually inverse maps are smooth, proving the assertion. □

We call the pair $(M_{\mathfrak{R}}(z), M_{\mathfrak{I}}(z))$ the *Möbius coordinates* of z. The theorem supplies global coordinates adapted to the ordered Möbius representation.

Next, we point out the relation between the Möbius coordinate system and the classical Lobachevsky coordinates for the hyperbolic plane [24,25]. Let $z \in \mathbb{D}$, and write $z = r \oplus_M si$, where $r = M_{\mathfrak{R}}(z)$ and $s = M_{\mathfrak{I}}(z)$. By the Möbius-Coordinate Map Theorem, the pair $(r, s) \in (-1, 1)^2$ is uniquely determined by z. We use the curvature -1 normalization and the following convention for *Lobachevsky coordinates* in the hyperboloid model:

$$(\lambda, \phi) \longmapsto (\sinh\lambda \cosh\phi, \sinh\phi, \cosh\lambda \cosh\phi).$$

Here, λ is the signed distance along the base geodesic and ϕ is signed perpendicular distance from it. This displayed convention fixes the order and signs of the parameters, which can differ between accounts of Lobachevsky coordinates. Then, the two coordinate systems are related by

$$r = \tanh\left(\frac{\lambda}{2}\right) \qquad \text{and} \qquad s = \tanh\left(\frac{\phi}{2}\right).$$

Equivalently, $\lambda = 2\tanh^{-1}(r)$ and $\phi = 2\tanh^{-1}(s)$. Indeed, since $r \oplus_M si = \dfrac{r + si}{1 + rsi}$, a direct computation gives $r \oplus_M si = \dfrac{r(1+s^2)}{1+r^2s^2} + \dfrac{s(1-r^2)}{1+r^2s^2}i$. Consider the hyperboloid model $\mathbb{H}^2 = \{(x, y, t) \in \mathbb{R}^3 : x^2 + y^2 - t^2 = -1,\ t > 0\}$. Under the usual correspondence from the Poincaré disk to this hyperboloid model (see Section 4.5 of [3]),

$$x + yi \longmapsto \left(\frac{2x}{1-x^2-y^2}, \frac{2y}{1-x^2-y^2}, \frac{1+x^2+y^2}{1-x^2-y^2}\right),$$

the point $r \oplus_M si$ is represented by

$$\left(\frac{2r(1+s^2)}{(1-r^2)(1-s^2)}, \frac{2s}{1-s^2}, \frac{(1+r^2)(1+s^2)}{(1-r^2)(1-s^2)}\right). \tag{10}$$

Using the identities $\sinh\left(2\tanh^{-1}(t)\right) = \dfrac{2t}{1-t^2}$ and $\cosh\left(2\tanh^{-1}(t)\right) = \dfrac{1+t^2}{1-t^2}$, we obtain that triple (10) becomes $(\sinh(\lambda)\cosh(\phi), \sinh(\phi), \cosh(\lambda)\cosh(\phi))$, which is the usual expression for Lobachevsky coordinates in the hyperboloid model. Hence, the Möbius coordinate system may be regarded as a bounded reparametrization of the Lobachevsky coordinates in the Poincaré disk, with the coordinate parameters expressed directly in terms of Möbius addition. The purpose of the Möbius-Coordinate Map Theorem is therefore not merely to obtain a global parametrization of the hyperbolic plane, but to describe this coordinate structure explicitly in terms of the Möbius real and imaginary parts arising from the orthogonal gyrodecomposition of the disk.

Now, we collect a few properties of $M_{\mathfrak{R}}$ and $M_{\mathfrak{I}}$, similar to properties of Re and Im. Let $z \in \mathbb{D}$. Using the identity $\mathrm{Re}(z) + \mathrm{Im}(z)i = M_{\mathfrak{R}}(z) \oplus_M M_{\mathfrak{I}}(z)i$, we obtain that

$$\mathrm{Re}(z) = \frac{(1 + M_{\mathfrak{I}}(z)^2)M_{\mathfrak{R}}(z)}{1 + M_{\mathfrak{R}}(z)^2 M_{\mathfrak{I}}(z)^2} \tag{11}$$

and

$$\mathrm{Im}(z) = \frac{(1 - M_{\mathfrak{R}}(z)^2)M_{\mathfrak{I}}(z)}{1 + M_{\mathfrak{R}}(z)^2 M_{\mathfrak{I}}(z)^2} \tag{12}$$

for all $z \in \mathbb{D}$. This implies that

$$|z| = \sqrt{M_{\mathfrak{R}}(z)^2 \oplus_M M_{\mathfrak{I}}(z)^2} \tag{13}$$

for all $z \in \mathbb{D}$. Here, the real numbers $M_{\mathfrak{R}}(z)^2, M_{\mathfrak{I}}(z)^2 \in [0, 1)$ are regarded as elements of the real diameter L_1. Thus, the operation in Equation (13) is the real restriction of Möbius addition, and the formula means

$$|z| = \sqrt{\frac{M_{\mathfrak{R}}(z)^2 + M_{\mathfrak{I}}(z)^2}{1 + M_{\mathfrak{R}}(z)^2 M_{\mathfrak{I}}(z)^2}},$$

with the nonnegative real square root. It follows also that

$$1 - |z|^2 = \frac{(1 - M_{\mathfrak{R}}(z)^2)(1 - M_{\mathfrak{I}}(z)^2)}{1 + M_{\mathfrak{R}}(z)^2 M_{\mathfrak{I}}(z)^2}. \tag{14}$$

4. Equivalence Relations Induced by $M_{\mathfrak{R}}$ and $M_{\mathfrak{I}}$

The partition framework is inherited from the orthogonal gyrodecomposition in [18] (Section 4.2, Equation (64) and Theorem 23); here we express the fibers explicitly and distinguish their geometric types using the coordinates of Section 3. For related work on curve families in Möbius gyrovector spaces, see the study of cogyrolines in [26]. Here, we determine the geometric types of our fibers directly. In fact, we introduce the equivalence relations induced by $M_{\mathfrak{R}}$ and $M_{\mathfrak{I}}$, motivated by the geometric structure of Euclidean lines. We begin by defining relations $\sim_{M_{\mathfrak{R}}}$ and $\sim_{M_{\mathfrak{I}}}$ on the Poincaré disk by the following conditions:

$$z \sim_{M_{\mathfrak{R}}} w \quad \Leftrightarrow \quad M_{\mathfrak{R}}(z) = M_{\mathfrak{R}}(w) \tag{15}$$

and

$$z \sim_{M_{\mathfrak{I}}} w \quad \Leftrightarrow \quad M_{\mathfrak{I}}(z) = M_{\mathfrak{I}}(w) \tag{16}$$

for all $z, w \in \mathbb{D}$. It is clear that $\sim_{M_{\mathfrak{R}}}$ and $\sim_{M_{\mathfrak{I}}}$ are equivalence relations on the Poincaré disk because they are defined via equality. The following two propositions describe the equivalence classes determined by $\sim_{M_{\mathfrak{R}}}$ and $\sim_{M_{\mathfrak{I}}}$, respectively.

Proposition 3. *Let $z \in \mathbb{D}$. Suppose that $[z]_{M_{\mathfrak{R}}}$ is the equivalence class containing z induced by $\sim_{M_{\mathfrak{R}}}$. Then,*

$$[z]_{M_{\mathfrak{R}}} = M_{\mathfrak{R}}(z) \oplus_M L_i. \tag{17}$$

Proof. Let $w \in [z]_{M_{\mathfrak{R}}}$. Then, $w \sim_{M_{\mathfrak{R}}} z$, and so $M_{\mathfrak{R}}(w) = M_{\mathfrak{R}}(z)$. By definition, $w = M_{\mathfrak{R}}(w) \oplus_M M_{\mathfrak{I}}(w)i$. Hence, $w = M_{\mathfrak{R}}(z) \oplus_M M_{\mathfrak{I}}(w)i \in M_{\mathfrak{R}}(z) \oplus_M L_i$. This proves that $[z]_{M_{\mathfrak{R}}} \subseteq M_{\mathfrak{R}}(z) \oplus_M L_i$. To prove the reverse inclusion, suppose that $w = M_{\mathfrak{R}}(z) \oplus_M si$ for some $s \in (-1, 1)$. By Proposition 2, $M_{\mathfrak{R}}(w) = M_{\mathfrak{R}}(M_{\mathfrak{R}}(z) \oplus_M si) = M_{\mathfrak{R}}(z)$, and so $w \sim_{M_{\mathfrak{R}}} z$. Thus, $w \in [z]_{M_{\mathfrak{R}}}$. □

It turns out that Equation (17) defines hyperbolic lines in the Poincaré disk model for two-dimensional hyperbolic geometry, as we will see shortly. Figure 2 illustrates hyperbolic lines whose representatives are chosen to be points on the real axis of the complex plane lying in the Poincaré disk.

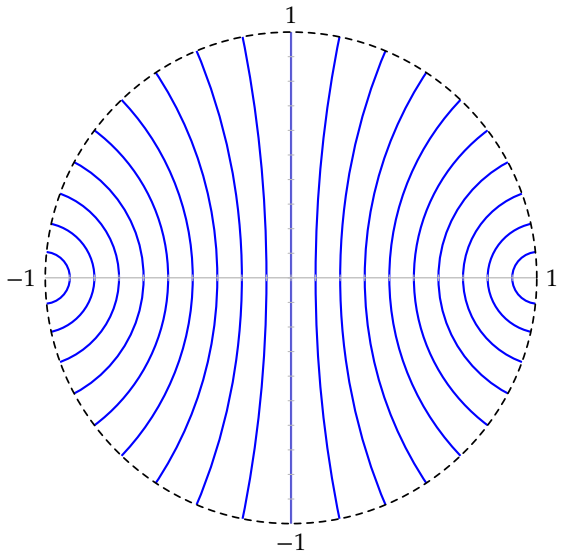

Figure 2. Examples of hyperbolic lines with representatives chosen to be points on the real axis of the complex plane lying in the Poincaré disk. The points on each line share the same Möbius real part.

Proposition 4. *Let $z \in \mathbb{D}$. Suppose that $[z]_{M_\mathfrak{I}}$ is the equivalence class containing z induced by $\sim_{M_\mathfrak{I}}$. Then,*

$$[z]_{M_\mathfrak{I}} = L_1 \oplus_M M_\mathfrak{I}(z)i. \tag{18}$$

Proof. Put $s = M_\mathfrak{I}(z)$. If $w \in [z]_{M_\mathfrak{I}}$, then $M_\mathfrak{I}(w) = s$ and the coordinate representation gives $w = M_\mathfrak{R}(w) \oplus_M si \in L_1 \oplus_M si$. Conversely, if $w = t \oplus_M si$ with $t \in L_1$, uniqueness in Theorem 1 gives $M_\mathfrak{I}(w) = s = M_\mathfrak{I}(z)$, and so $w \in [z]_{M_\mathfrak{I}}$. Both inclusions prove the equality. □

A geometric aspect of equivalence classes given by Equation (18) is illustrated in Figure 3. The ordering explains the difference between the two families. Fixing $r = M_\mathfrak{R}(z)$ gives $\tau_r(L_i)$, the image of a diameter under a single left translation. Fixing $s = M_\mathfrak{I}(z)$ gives $\{t \oplus_M si : t \in (-1, 1)\}$, in which the left operand varies. Noncommutativity prevents replacement of this set by $\tau_{si}(L_1)$. This distinction concerns the roles of the two ordered operands. For an explicit geometric description, write a point of the latter set as $x + yi$. Its inverse-coordinate equation gives $y = s(1 - x^2 - y^2)/(1 - s^2)$. If $s = 0$, this is the real diameter. If $s \neq 0$, it is the part in $\mathbb{D}$ of the circle

$$x^2 + y^2 + \frac{1 + s^2}{s} y - 1 = 0. \tag{19}$$

Its center is $(0, -(1 - s^2)/(2s))$, and its radius is $(1 + s^2)/(2|s|)$. The square of the radius exceeds the square of the distance of the center from the origin by 1, so the condition for orthogonality to the unit circle is not satisfied. Accordingly, nonzero $M_\mathfrak{I}$ level sets are not hyperbolic lines. In the Lobachevsky convention above, they are curves of constant signed distance from the real diameter, as established in Section 5.

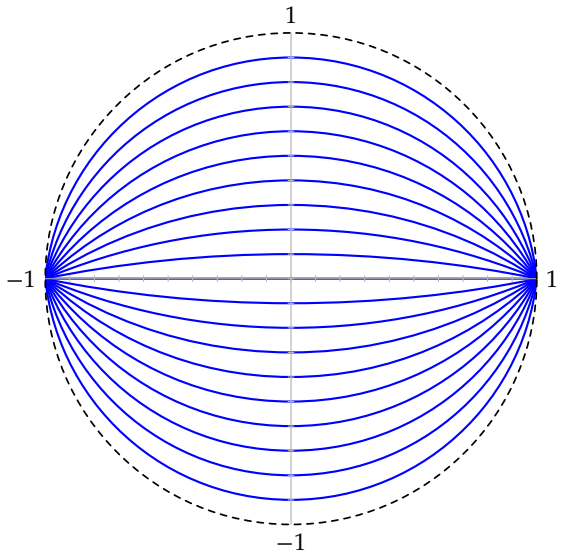

Figure 3. Examples of equivalence classes given by Equation (18) with representatives chosen to be points on the imaginary axis of the complex plane lying in the Poincaré disk. The points on each curve share the same Möbius imaginary part.

Next, we extend Propositions 3 and 4 to the case of more general axes. Fix $\omega \in \mathbb{S}^1$, and let $z \in \mathbb{D}$. Note that $\overline{\omega}z$ lies in $\mathbb{D}$. Since $\overline{\omega}z = z/\omega$, we apply the standard-axis representation to this rotated point. We have $\overline{\omega}z = M_{\Re}(\overline{\omega}z) \oplus_M M_{\Im}(\overline{\omega}z)i$. Multiplying by ω and applying Formula (2) gives

$$z = M_{\Re}(\overline{\omega}z)\omega \oplus_M M_{\Im}(\overline{\omega}z)\omega i. \tag{20}$$

According to Proposition 1, $(M_{\Re}(\overline{\omega}z)\omega, M_{\Im}(\overline{\omega}z)\omega i)$ is the unique pair in $L_\omega \times L_{\omega i}$ such that $z = M_{\Re}(\overline{\omega}z)\omega \oplus_M M_{\Im}(\overline{\omega}z)\omega i$. This allows us to define two functions on the Poincaré disk as follows:

$$\mathcal{P}^{\ell}_{\omega}(z) = M_{\Re}(\overline{\omega}z)\omega \tag{21}$$

and

$$\mathcal{P}^{r}_{\omega}(z) = M_{\Im}(\overline{\omega}z)\omega i \tag{22}$$

for all $z \in \mathbb{D}$. By definition, $z = \mathcal{P}^{\ell}_{\omega}(z) \oplus_M \mathcal{P}^{r}_{\omega}(z)$, and furthermore $\mathcal{P}^{\ell}_{\omega}(z) \perp \mathcal{P}^{r}_{\omega}(z)$. More precisely, $\mathcal{P}^{\ell}_{\omega} : \mathbb{D} \to L_\omega$ and $\mathcal{P}^{r}_{\omega} : \mathbb{D} \to L_{\omega i}$ select the factors in the unique ordered representation. Each restricts to the identity on its target diameter. Their construction follows from rotational covariance, and $\perp$ here refers to Euclidean orthogonality of the two factors. The rotation back to the standard axes is $\overline{\omega}z$, not ωz; for example, when $\omega = i$ it is $-iz$, and multiplying back by i recovers z. We pay particular attention to the function $\mathcal{P}^{\ell}_{\omega}$, as it induces hyperbolic lines in a manner similar to Proposition 3.

Proposition 5. *Let $\omega \in \mathbb{S}^1$, and let $a, b \in \mathbb{D}$. Then, $\mathcal{P}^{\ell}_{\omega}(a) = \mathcal{P}^{\ell}_{\omega}(b)$ if and only if $-\mathcal{P}^{\ell}_{\omega}(b) \oplus_M a$ lies in $L_{\omega i}$.*

Proof. Put $p = \mathcal{P}^{\ell}_{\omega}(b) \in L_\omega$. If $\mathcal{P}^{\ell}_{\omega}(a) = p$, then $a = p \oplus_M \mathcal{P}^{r}_{\omega}(a)$. The first identity in Equation (3) gives $(-p) \oplus_M a = \mathcal{P}^{r}_{\omega}(a) \in L_{\omega i}$. Conversely, suppose $q = (-p) \oplus_M a \in L_{\omega i}$. The second identity in Equation (3) gives $a = p \oplus_M q$. Since $(p, q) \in L_\omega \times L_{\omega i}$, uniqueness in Proposition 1 gives $\mathcal{P}^{\ell}_{\omega}(a) = p = \mathcal{P}^{\ell}_{\omega}(b)$. This proves the proposition. □

In light of Proposition 5, we obtain another equivalence relation on the Poincaré disk, denoted by $\sim_\omega$, given by the condition that

$$a \sim_\omega b \quad \Leftrightarrow \quad -\mathcal{P}^\ell_\omega(b) \oplus_M a \in L_{\omega i} \tag{23}$$

for all $a, b \in \mathbb{D}$. This is an equivalence relation because the preceding proposition identifies it with equality of the values of $\mathcal{P}^\ell_\omega$. The following proposition gives an algebraic description of equivalence classes determined by condition (23).

Proposition 6. *Let $z \in \mathbb{D}$. Suppose that $[z]_\omega$ is the equivalence class containing z induced by $\sim_\omega$. Then,*

$$[z]_\omega = \mathcal{P}^\ell_\omega(z) \oplus_M L_{\omega i}. \tag{24}$$

Proof. Suppose that $w \in [z]_\omega$. Then, $w \sim_\omega z$, and so $\mathcal{P}^\ell_\omega(w) = \mathcal{P}^\ell_\omega(z)$. This implies that $w = \mathcal{P}^\ell_\omega(z) \oplus_M \mathcal{P}^r_\omega(w) \in \mathcal{P}^\ell_\omega(z) \oplus_M L_{\omega i}$. This proves the inclusion $[z]_\omega \subseteq \mathcal{P}^\ell_\omega(z) \oplus_M L_{\omega i}$. To prove the reverse inclusion, suppose that $w \in \mathcal{P}^\ell_\omega(z) \oplus_M L_{\omega i}$. Then, $w = \mathcal{P}^\ell_\omega(z) \oplus_M c$ for some $c \in L_{\omega i}$. By the uniqueness of expression of w as a Möbius sum, $\mathcal{P}^\ell_\omega(w) = \mathcal{P}^\ell_\omega(z)$, and so $w \sim_\omega z$. Thus, $w \in [z]_\omega$, and so equality holds. □

We use the following standard Möbius-geometric fact, included for completeness; see [2]. Orthogonality to $\mathbb{S}^1$ below means Euclidean orthogonality of the boundary circles or lines, which is preserved by conformal transformations and defines geodesics in the Poincaré disk.

Lemma 1. *Let $a \in \mathbb{D}$. If L is a hyperbolic line, then $\tau_a(L)$ is a hyperbolic line.*

Proof. The map τ_a is an invertible Möbius transformation with inverse τ_{-a} by left cancellation laws in Equation (3). Formula (4) gives $\tau_a(\mathbb{D}) = \mathbb{D}$ and, upon extending to the boundary, $\tau_a(\mathbb{S}^1) = \mathbb{S}^1$. Its pole is outside the closed disk when $a \neq 0$, and the case when $a = 0$ gives the identity transformation. Write $L = C \cap \mathbb{D}$, where C is a generalized circle orthogonal to $\mathbb{S}^1$. Möbius transformations preserve generalized circles and angles, so $\tau_a(C)$ is orthogonal to $\mathbb{S}^1$. Since τ_a is bijective and preserves $\mathbb{D}$, $\tau_a(L) = \tau_a(C) \cap \mathbb{D}$, which is the entire hyperbolic line determined by $\tau_a(C)$. □

Figure 4 illustrates this standard fact through the factorization in Equation (5). Its relevance to the coordinate theory is that every fiber in Equation (24) is the image of an orthogonal diameter under a fixed left translation. The six panels visualize the mechanism behind this geometric description, rather than an additional coordinate-map result.

Proposition 7. *Let $z \in \mathbb{D}$, and let $\omega \in \mathbb{S}^1$. Suppose that $[z]_\omega$ is the equivalence class containing z induced by $\sim_\omega$. Then, $[z]_\omega$ is a hyperbolic line passing through z and $\mathcal{P}^\ell_\omega(z)$.*

Proof. Note that $L_{\omega i}$ is a hyperbolic line since it is a diameter of the Poincaré disk. Since $[z]_\omega = \tau_{\mathcal{P}^\ell_\omega(z)}(L_{\omega i})$, it follows from Lemma 1 that $[z]_\omega$ is a hyperbolic line because it is the image of a hyperbolic line under the Möbius translation $\tau_{\mathcal{P}^\ell_\omega(z)}$. The decomposition $z = \mathcal{P}^\ell_\omega(z) \oplus_M \mathcal{P}^r_\omega(z)$ shows that z belongs to this image, while $\mathcal{P}^\ell_\omega(z) = \tau_{\mathcal{P}^\ell_\omega(z)}(0)$ shows membership of the projected point. These two points may coincide when z lies in L_ω. □

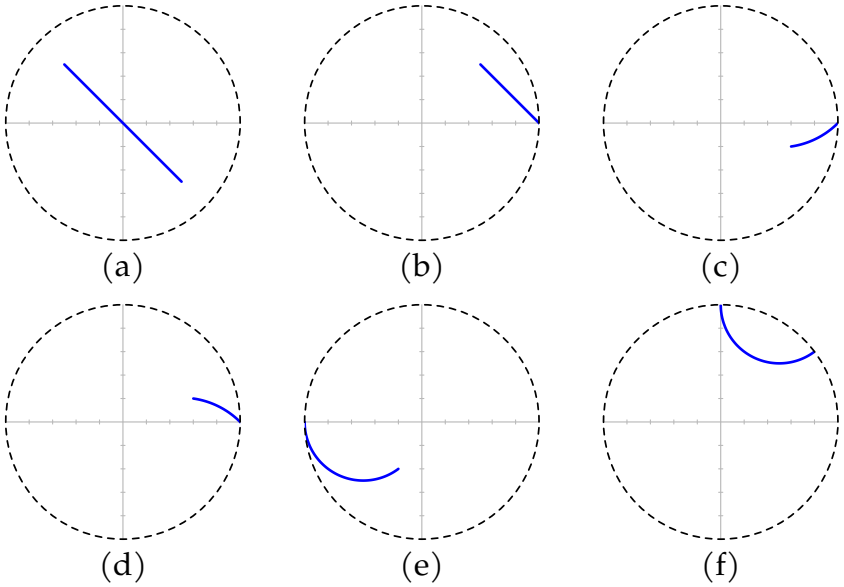

Figure 4. Let $a = 0.5 + 0.5i$. (**a**) Transforming L_1 using $\rho_{\overline{a}}$; (**b**) Transforming $\rho_{\overline{a}}(L_1)$ using T_1; (**c**) Transforming $T_1(\rho_{\overline{a}}(L_1))$ using $\iota_{\mathbb{S}^1}$; (**d**) Transforming $\iota_{\mathbb{S}^1}(T_1(\rho_{\overline{a}}(L_1)))$ using κ; (**e**) Transforming $\kappa(\iota_{\mathbb{S}^1}(T_1(\rho_{\overline{a}}(L_1))))$ using $\rho_{\frac{|a|^2-1}{|a|^2}a}$; (**f**) Transforming $\rho_{\frac{|a|^2-1}{|a|^2}a}(\kappa(\iota_{\mathbb{S}^1}(T_1(\rho_{\overline{a}}(L_1)))))$ using $T_{\frac{a}{|a|^2}}$, which is the hyperbolic line $\tau_a(L_1)$. The hyperbolic line in each panel is shown in blue.

5. Perpendicular Projection and Distance in Möbius Coordinates

We now apply the coordinate formulas to metric projection onto a diameter. The nearest-point and distance identities below are coordinate expressions of standard hyperbolic geometry [4,24]. Other metric constructions in the Poincaré disk include the hyperbolic Carnot theorem [27] and the hyperbolic Stewart and Steiner theorems [28]; our application concerns the problem of a perpendicular foot and its distance to a given point. The Möbius real part determines the perpendicular foot, whereas the Möbius imaginary part determines the signed perpendicular distance. We use the Poincaré metric of curvature -1 [3], given by

$$d(z,w) = 2\tanh^{-1}\left(\frac{|z-w|}{|1-\overline{z}w|}\right), \qquad z,w \in \mathbb{D}.$$

For a nonempty subset $S \subseteq \mathbb{D}$, write $d(z,S) = \inf_{w\in S} d(z,w)$.

Theorem 3 (Nearest-Point Property)**.** *For $z \in \mathbb{D}$, the unique nearest point to z on the real diameter L_1 is $M_{\mathfrak{R}}(z)$. The distance is equal to*

$$d(z,L_1) = 2\tanh^{-1}(|M_{\mathfrak{I}}(z)|) = \sinh^{-1}\left(\frac{2|\mathrm{Im}(z)|}{1-|z|^2}\right). \tag{25}$$

More generally, for $\omega \in \mathbb{S}^1$, the nearest point on L_ω is $\mathcal{P}^{\ell}_{\omega}(z)$ and

$$d(z,L_\omega) = 2\tanh^{-1}(|M_{\mathfrak{I}}(\overline{\omega}z)|) = \sinh^{-1}\left(\frac{2|\mathrm{Im}(\overline{\omega}z)|}{1-|z|^2}\right). \tag{26}$$

Proof. Fix $z \in \mathbb{D}$, and put $x = \mathrm{Re}(z)$, $\rho = |z|^2$, $r = M_{\mathfrak{R}}(z)$, and $s = M_{\mathfrak{I}}(z)$. For $t \in (-1,1)$, define

$$F_z(t) = |(-z) \oplus_M t|^2 = \frac{t^2 - 2xt + \rho}{\rho t^2 - 2xt + 1}.$$

The denominator is $|1-\overline{z}t|^2 > 0$. Furthermore, $1 - F_z(t) = \dfrac{(1-\rho)(1-t^2)}{\rho t^2 - 2xt + 1} > 0$, and so $0 \le F_z(t) < 1$. Differentiation gives

$$F_z'(t) = \frac{2(1-\rho)q(t)}{(\rho t^2 - 2xt + 1)^2}, \qquad q(t) = -xt^2 + (1+\rho)t - x.$$

In the case when $x = 0$, $t = 0$ is the unique critical point of F_z. Hence, F_z attains a local minimum at $t = 0 = r$ by the first derivative test. Now, suppose that $x \neq 0$. As in the proof of Theorem 1, $q(r) = 0$. Moreover, for every $t \in (-1, 1)$,

$$q'(t) = 1 + \rho - 2xt \ge 1 + \rho - 2|x| = (1 - |x|)^2 + (\mathrm{Im}(z))^2 > 0.$$

Thus, $q(t) < 0$ for $t < r$ and $q(t) > 0$ for $t > r$. Since $1 - \rho > 0$, the same signs hold for $F_z'(t)$. Consequently, F_z is strictly decreasing on $(-1, r)$ and strictly increasing on $(r, 1)$, and so r is its unique global minimizer. The identity $d(z,t) = 2\tanh^{-1}\sqrt{F_z(t)}$ and the strict monotonicity of the square root and inverse hyperbolic tangent functions show that r is also the unique nearest point to z on L_1.

To compute the minimum distance, use $z = r \oplus_M si$ and the first identity in Equation (3) to obtain $(-r) \oplus_M z = si$. Since r is real,

$$\sqrt{F_z(r)} = \frac{|z-r|}{|1-\overline{z}r|} = \frac{|z-r|}{|1-rz|} = |(-r) \oplus_M z| = |s|.$$

Hence, $d(z, L_1) = 2\tanh^{-1}(|s|)$. As in the proof of Theorem 2 and Equation (14),

$$\mathrm{Im}(z) = \frac{s(1-r^2)}{1+r^2s^2} \qquad \text{and} \qquad 1 - |z|^2 = \frac{(1-r^2)(1-s^2)}{1+r^2s^2}.$$

Hence, $\dfrac{2|\mathrm{Im}(z)|}{1-|z|^2} = \dfrac{2|s|}{1-s^2} = \sinh\Big(2\tanh^{-1}(|s|)\Big)$, which proves the second expression in Equation (25).

For perpendicularity, the Möbius translation τ_r maps L_i to the hyperbolic line $r \oplus_M L_i$ through z and r, and maps L_1 onto itself. It is conformal, so the right angle between L_i and L_1 at 0 becomes a right angle between $r \oplus_M L_i$ and L_1 at r. Finally, the rotation $z \mapsto \overline{\omega}z$ preserves the Poincaré distance and sends L_ω onto L_1. Applying the result to $\overline{\omega}z$ and rotating back gives the unique nearest point $M_{\Re}(\overline{\omega}z)\omega = \mathcal{P}_\omega^\ell(z)$ and the stated distance to L_ω. □

Theorem 3 gives a metric interpretation of both coordinate families. By Proposition 3, a fiber with fixed $M_{\Re}(z) = r$ is the perpendicular geodesic $r \oplus_M L_i$ through r. To specify signed distance, take the upper half of the disk as the positive side of L_1 and the lower half as the negative side, with signed distance zero on L_1. The formula for $\mathrm{Im}(z)$ in the proof shows that $\mathrm{Im}(z)$ and $s = M_{\Im}(z)$ have the same sign. Hence, the signed distance is

$$\delta(z, L_1) = 2\tanh^{-1}(M_{\Im}(z)) = \sinh^{-1}\left(\frac{2\mathrm{Im}(z)}{1-|z|^2}\right). \tag{27}$$

Thus, a fiber with fixed $M_{\Im}(z) = s$ is a curve of constant signed distance $\phi = 2\tanh^{-1}(s)$, consistently with the Lobachevsky convention in Section 3. For $s \neq 0$, these curves are hypercycles; for $s = 0$, the fiber is L_1. The ordered factors therefore have different roles: r is the metric projection onto L_1, while si represents perpendicular displacement and is generally not the metric projection onto L_i.

https://doi.org/10.3390/math14213971

Example 1. *Let* $z = (1+i)/2$. *Then,* $|z|^2 = 1/2$, *and Equations* (7) *and* (8) *give*

$$M_{\mathfrak{R}}(z) = \frac{2}{3+\sqrt{5}} = \frac{3-\sqrt{5}}{2} \qquad \text{and} \qquad M_{\mathfrak{I}}(z) = \frac{2}{1+\sqrt{5}} = \frac{\sqrt{5}-1}{2}.$$

Thus, the perpendicular foot on the real diameter is $(3-\sqrt{5})/2$, *and the distance to it is*

$$d(z, L_1) = \sinh^{-1}(2) = \log(2+\sqrt{5}).$$

The foot differs from the Euclidean real part $1/2$. *This example also illustrates the asymmetry of the ordered factors. Taking* $\omega = i$ *in Theorem 3, the nearest point on* L_i *is*

$$\mathcal{P}_i^{\ell}(z) = M_{\mathfrak{R}}(-iz)i = \frac{3-\sqrt{5}}{2}i,$$

which differs from the second factor $M_{\mathfrak{I}}(z)i = (\sqrt{5}-1)i/2$. *Thus, the coordinate formulas give the perpendicular foot and distance directly, without solving for a circle center or intersecting geodesics. This application makes the explicit scalar realization useful for calculation; the underlying metric projection principle is standard hyperbolic geometry. Indeed, for a specified diameter* L_ω, *the same procedure first rotates the input to* $\overline{\omega}z$, *evaluates the two scalar Formulas* (7) *and* (8), *and rotates the foot back. Thus, one pair of scalar evaluations provides both the foot and the perpendicular displacement, while avoiding the mistaken identification of the second ordered factor with projection onto the perpendicular diameter. This is a convenience of representation and interpretation.*

6. Conclusions

We have expressed the known orthogonal Möbius gyrodecomposition [18] in the complex disk through explicit scalar functions $M_{\mathfrak{R}}$ and $M_{\mathfrak{I}}$. Their ordered reconstruction map gives a diffeomorphism $\mathbb{D} \cong (-1,1)^2$, and the corresponding parameters are bounded reparametrizations of Lobachevsky coordinates in the stated convention. The level sets distinguish perpendicular geodesics from curves of constant signed distance, and rotational covariance gives the formulas along any diameter. The perpendicular-foot and distance calculation illustrates how this scalar realization turns a geometric construction into a direct computation in the disk. This explicit-coordinate viewpoint is relevant to the broader settings of numerical hyperbolic geometry [29] and hyperbolic graph visualization [30]. Lobachevsky coordinates also appear in the study of flexible hyperbolic bipartite frameworks [25]; applying the present formulas in these settings would require separate investigation.

The general orthogonal gyrodecomposition and the underlying projection framework are already established in [18]; the present contribution is their explicit two-dimensional coordinate treatment and its geometric interpretation. Possible further work includes similarly explicit coordinate descriptions in higher-dimensional Möbius gyrovector spaces and computational uses of the resulting projection formulas. Such extensions require analysis beyond the two-factor complex formulas used here.

Author Contributions: Conceptualization, T.S.; Methodology, T.S.; Validation, W.A., J.W., W.S. and T.S.; Investigation, W.A., J.W., W.S. and T.S.; Writing—Original Draft, T.S.; Writing—Review & Editing, W.A., J.W. and W.S.; Project Administration, T.S. All authors have read and agreed to the published version of the manuscript.

Funding: Teerapong Suksumran was financially supported by the CMU Mid-Career Research Fellowship program, Chiang Mai University, under grant number MRCMUR2569_(22).

Data Availability Statement: No new data were created or analyzed in this study. Data sharing is not applicable to this article.

Acknowledgments: We are grateful to Tarid Suwansri for his collaboration in the computational and graphical parts. We sincerely thank the referees for their careful reading of our manuscript and their constructive comments and suggestions. Their feedback has helped us clarify the contribution, strengthen the proofs, and improve the exposition and geometric interpretation of the results. Also, Teerapong Suksumran thanks Keiichi Watanabe for his kind hospitality and for hosting his research visit to Niigata University. The authors used OpenAI Codex (GPT-6) to assist with language editing, reorganization of mathematical proofs, and development of a worked geometric example. The authors reviewed and edited the generated material, independently verified the mathematical statements and proofs, and take full responsibility for the content of this publication.

Conflicts of Interest: The authors declare no conflicts of interest.

References

1. Dillon, M. *Geometry Through History: Euclidean, Hyperbolic, and Projective Geometries*; Springer: Cham, Switzerland, 2018. [CrossRef]
2. Hitchman, M. *Geometry with an Introduction to Cosmic Topology*; CreateSpace Independent Publishing Platform: North Charleston, SC, USA, 2018.
3. Ratcliffe, J. *Foundations of Hyperbolic Manifolds*, 3rd ed.; Graduate Texts in Mathematics; Springer: Cham, Switzerland, 2019; Volume 149. [CrossRef]
4. Anderson, J. *Hyperbolic Geometry*, 2nd ed.; Springer Undergraduate Mathematics Series; Springer: London, UK, 2005. [CrossRef]
5. Ungar, A. *Analytic Hyperbolic Geometry and Albert Einstein's Special Theory of Relativity*; World Scientific: Hackensack, NJ, USA, 2008. [CrossRef]
6. Ungar, A. *A Gyrovector Space Approach to Hyperbolic Geometry*; Synthesis Lectures on Mathematics & Statistics; Springer: Cham, Switzerland, 2009. [CrossRef]
7. Ungar, A. From Möbius to gyrogroups. *Amer. Math. Mon.* **2008**, *115*, 138–144. [CrossRef]
8. Ungar, A. *Beyond the Einstein Addition Law and Its Gyroscopic Thomas Precession: The Theory of Gyrogroups and Gyrovector Spaces*; Fundamental Theories of Physics; Springer: Dordrecht, The Netherlands, 2002; Volume 11. [CrossRef]
9. Ungar, A. Einstein's velocity addition law and its hyperbolic geometry. *Comput. Math. Appl.* **2007**, *53*, 1228–1250. [CrossRef]
10. Kim, S.; Lawson, J. Unit balls, Lorentz boosts, and hyperbolic geometry. *Results Math.* **2013**, *63*, 1225–1242. [CrossRef]
11. Ungar, A. The hyperbolic geometric structure of the density matrix for mixed state qubits. *Found. Phys.* **2002**, *32*, 1671–1699. [CrossRef]
12. Ungar, A. *Barycentric Calculus in Euclidean and Hyperbolic Geometry: A Comparative Introduction*; World Scientific: Hackensack, NJ, USA, 2010. [CrossRef]
13. Ungar, A. The hyperbolic triangle centroid. *Comment. Math. Univ. Carol.* **2004**, *45*, 355–369.
14. Ungar, A. The hyperbolic square and Möbius transformations. *Banach J. Math. Anal.* **2007**, *1*, 101–116. [CrossRef]
15. Birman, S.; Ungar, A. The hyperbolic derivative in the Poincaré ball model of hyperbolic geometry. *J. Math. Anal. Appl.* **2001**, *254*, 321–333. [CrossRef]
16. Ferreira, M. Harmonic analysis on the Möbius gyrogroup. *J. Fourier Anal. Appl.* **2015**, *21*, 281–317. [CrossRef]
17. Barabanov, N.; Ungar, A. Binary Operations in the Unit Ball: A Differential Geometry Approach. *Symmetry* **2020**, *12*, 1178. [CrossRef]
18. Ferreira, M.; Suksumran, T. Orthogonal gyrodecompositions of real inner product gyrogroups. *Symmetry* **2020**, *12*, 941. [CrossRef]
19. Suksumran, T. The algebra of gyrogroups: Cayley's theorem, Lagrange's theorem, and isomorphism theorems. In *Essays in Mathematics and Its Applications*; Rassias, T.M., Pardalos, P.M., Eds.; Springer: Cham, Switzerland, 2016; pp. 369–437. [CrossRef]
20. Ferreira, M. Factorizations of Möbius gyrogroups. *Adv. Appl. Clifford Algebr.* **2009**, *19*, 303–323. [CrossRef]
21. Ferreira, M.; Ren, G. Möbius gyrogroups: A Clifford algebra approach. *J. Algebra* **2011**, *328*, 230–253. [CrossRef]
22. Watanabe, K. Orthogonal gyroexpansion in Möbius gyrovector spaces. *J. Funct. Spaces* **2017**, *2017*, 1518254. [CrossRef]
23. Maungchang, R.; Atiponrat, W.; Suwansri, T.; Wattanapan, J.; Suksumran, T. The complete list of solutions to Möbius's exponential equation. *Eur. J. Pure Appl. Math.* **2025**, *18*, 6041. [CrossRef]
24. Smogorzhevsky, A. *Lobachevskian Geometry*; Mir Publishers: Moscow, Russia, 1982.
25. Kovalev, M.; Orevkov, S. Complete bipartite graphs flexible in the plane. *Sb. Math.* **2023**, *214*, 1390–1414. [CrossRef]
26. Demirel, O.; Seyrantepe, E. The cogyrolines of Möbius gyrovector spaces are metric but not periodic. *Aequat. Math.* **2013**, *85*, 185–200. [CrossRef]
27. Demirel, O.; Seyrantepe, E. The hyperbolic Carnot theorem in the Poincaré disc model of hyperbolic geometry. *Novi Sad J. Math.* **2008**, *38*, 33–39.
28. Demirel, O. The theorems of Stewart and Steiner in the Poincaré disc model of hyperbolic geometry. *Comment. Math. Univ. Carol.* **2009**, *50*, 359–371.

29. Celińska-Kopczyńska, D.; Kopczyński, E. Numerical Aspects of Hyperbolic Geometry. In *Computational Science—ICCS 2024*; Lecture Notes in Computer Science; Springer: Cham, Switzerland, 2024; Volume 14837, pp. 115–130. [CrossRef]
30. Miller, J.; Kobourov, S.; Huroyan, V. Browser-based Hyperbolic Visualization of Graphs. In *2022 IEEE 15th Pacific Visualization Symposium (PacificVis)*; IEEE: New York, NY, USA, 2022; pp. 71–80. [CrossRef]

Disclaimer/Publisher's Note: The statements, opinions and data contained in all publications are solely those of the individual author(s) and contributor(s) and not of MDPI and/or the editor(s). MDPI and/or the editor(s) disclaim responsibility for any injury to people or property resulting from any ideas, methods, instructions or products referred to in the content.